Structural basis for phosphoserine-proline recognition by group IV WW domains

Mark A. Verdecia[1,2], Marianne E. Bowman[1], Kun Ping Lu[3], Tony Hunter[4] and Joseph P. Noel[1]

[1]Structural Biology Laboratory and [2]Department of Biology, University of California, San Diego, La Jolla, California 92093, USA. [3]Department of Medicine, Harvard Medical School, Boston, Massachusetts 02215, USA. [4]Molecular Biology and Virology Laboratory, The Salk Institute for Biological Studies, La Jolla, California 92037, USA.

Pin1 contains an N-terminal WW domain and a C-terminal peptidyl-prolyl *cis-trans* isomerase (PPIase) domain connected by a flexible linker. To address the energetic and structural basis for WW domain recognition of phosphoserine (P.Ser)/phosphothreonine (P.Thr)- proline containing proteins, we report the energetic and structural analysis of a Pin1–phosphopeptide complex. The X-ray crystal structure of Pin1 bound to a doubly phosphorylated peptide (Tyr-P.Ser-Pro-Thr-P.Ser-Pro-Ser) representing a heptad repeat of the RNA polymerase II large subunit's C-terminal domain (CTD), reveals the residues involved in the recognition of a single P.Ser side chain, the rings of two prolines, and the backbone of the CTD peptide. The side chains of neighboring Arg and Ser residues along with a backbone amide contribute to recognition of P.Ser. The lack of widespread conservation of the Arg and Ser residues responsible for P.Ser recognition in the WW domain family suggests that only a subset of WW domains can bind P.Ser-Pro in a similar fashion to that of Pin1.

The WW domain is a 38–40 amino acid structural motif that functions as an interaction module in a diverse set of signaling proteins[1]. The modular nature of WW domain interactions lends itself to classification into five distinct groups based upon current understanding of their binding specificity. Group I WW domains, like those found in dystrophin and YAP65 (Yes kinase-associated protein), recognize 'PPxY' motifs[2] where x is any amino acid. Group II WW domains, like those of FE65 and formin binding proteins (FBPs), bind the 'PPLP' motif[3]. Group III WW domains, such as those found in a subset of FBPs, interact with 'PGM' motifs[4]. A fourth group, which includes the WW domain of Pin1, specifically interacts with P.Ser-Pro or P.Thr-Pro motifs[5]. The group V WW domains, including the WW domain of FBP30, recognize Pro-Arg motifs[6,7].

Pin1 has been implicated in the regulation of a diverse set of mitotically phosphorylated proteins, including Cdc25 (Cell division control Cdc2 phosphatase), Myt1 (Membrane-associated Tyr/Thr Cdc2 inhibiting kinase), Wee1 (Cdc2 kinase), Plk1 (Polo-like kinase), and Cdc27 (refs 8–10), and also Tau[11]. In addition, Pin1 and its homolog in *Saccharomyces cerevisiae*, Ess1p, have both been implicated in the regulation of the C-terminal domain (CTD) of RNA polymerase II (Pol II). Pin1's regulatory activity likely correlates with its ability to interact with this CTD, as both Pin1 and Ess1p have been shown to bind directly and preferentially to the phosphorylated form of the CTD[12–15]. Phosphorylation of Ser 2 and/or Ser 5 of the multiple Tyr-Ser 2-Pro-Thr-Ser 5-Pro-Ser heptad repeats found in the CTD of Pol II by cyclin dependent kinases (CDKs) initiates a cascade of transcriptional, processing, and splicing events linked to the elongating polymerase[16,17]. Recognition of these multiple repeats by the WW domains found in the E3 ubiquitin ligase, Rsp5 (reversion of Spt phenotype) is negatively regulated by phosphorylation[18]. On the other hand, Pin1 and Ess1p, which possess group IV WW domains, recognize and bind to the phosphorylated CTD.

Structural[19] and functional[20] analysis of Pin1 established that Pin1's C-terminal catalytic PPIase domain, which belongs to the parvulin family of PPIases, catalyzes phosphorylation dependent prolyl–peptide bond isomerization in P.Ser-Pro segments such as those found in the CTD of Pol II. More recent studies demonstrated that the Pin1 WW domain acts as the predominant P.Ser/P.Thr-Pro binding motif[5].

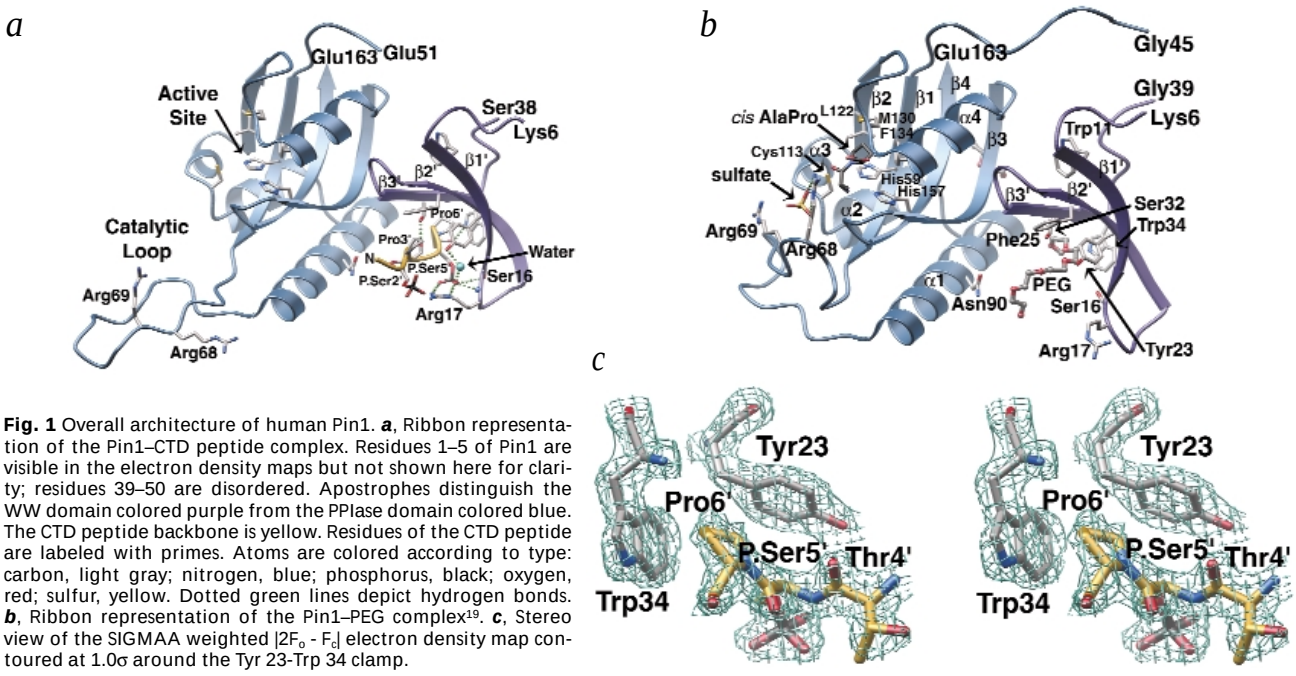

Fig. 1 Overall architecture of human Pin1. ***a***, Ribbon representation of the Pin1–CTD peptide complex. Residues 1–5 of Pin1 are visible in the electron density maps but not shown here for clarity; residues 39–50 are disordered. Apostrophes distinguish the WW domain colored purple from the PPIase domain colored blue. The CTD peptide backbone is yellow. Residues of the CTD peptide are labeled with primes. Atoms are colored according to type: carbon, light gray; nitrogen, blue; phosphorus, black; oxygen, red; sulfur, yellow. Dotted green lines depict hydrogen bonds. ***b***, Ribbon representation of the Pin1–PEG complex[19]. ***c***, Stereo view of the SIGMAA weighted $|2F_o - F_c|$ electron density map contoured at 1.0σ around the Tyr 23-Trp 34 clamp.

Table 1 Dissociation equilibrium constants (μM) for Pin1–peptide complexes[1]

Labeled peptide	Full-length Pin1	WW domain	PPIase catalytic domain
WFYSPFLE (Pintide)	> 540	N.d.	N.d.
WFYpSPFLE (Pintide)	17 ± 2.0	44 ± 9.5	86 ± 11
VPRpTPV (Cdc25c-T48)	4.9 ± 1.1	7.7 ± 3.3	N.b.
YLGpSPI (Cdc25c-S168)	69 ± 10	91 ± 30	> 400
LYRpSPS (Cdc25c-S214)	47 ± 7.3	72 ± 15	> 500
GSSpSPV (Wee1-S123)	73 ± 4.9	N.d.	N.d.
PPApTPP (Myt1-T412)	12 ± 2.1	15 ± 4.7	N.b.
PPGpSPP (Myt1-S416)	80 ± 18	126 ± 21	N.b.
STSpTPR (Myt1-T455)	46 ± 6.5	39 ± 12	N.b.
YSPTSPS (CTD)	N.b.	N.b.	N.b.
YpSPTSPS (CTD-S2)	61 ± 6.3	110 ± 26	N.b.
YSPTpSPS (CTD-S5)	30 ± 3.9	34 ± 5.9	> 500
YpSPTpSPS (CTD-S2/S5)	10 ± 0.83	34 ± 6.2	390 ± 82

[1]Errors are deviations from theoretical binding isotherms. All peptides were derived from human proteins except for Pintide. N.b., no detectable binding; N.d., not determined. The residues and phosphorylation sites are indicated with single letter amino acid codes and numbered according to sequences appearing in public data bases.

Binding analysis

We measured the affinity of full-length Pin1 and its isolated PPIase and WW domains for peptides labeled at their N-termini with rhodamine using fluorescence anisotropy. The measured dissociation constants (K_d) range from 5–80 μM for full-length Pin1 (Table 1). The peptides were derived from proteins previously shown to interact with Pin1. While the set of peptides examined is limited, a consensus emerges from comparison of the highest affinity interactions. The core binding element determined from this group of peptides is Pro-Xaa-P.Ser/P.Thr-Pro, where Xaa cannot be Gly. Surprisingly, the best binding sequences differ from the consensus Pin1 binding sequence of Trp-Phe-Tyr-P.Ser-Pro-Arg determined using a degenerate P.Ser-Pro anchored peptide library[20]. Furthermore, the dissociation constants roughly segregate into two affinity groups. The lower affinity interactions are more typical of other WW domain–peptide complexes, with K_d values > 50 μM. The higher affinity interactions possess K_d values < 35 μM.

For the Pol II CTD phosphopeptides, the degree of phosphorylation as well as the position of the P.Ser residues regulate their affinity for Pin1. The monophosphorylated P.Ser 5 peptide, which contains the minimal Pro-Xaa-P.Ser-Pro sequence, binds two-fold more tightly to Pin1 than the P.Ser 2 species, which lacks the N-terminal Pro. Phosphorylation of both Ser 2 and Ser 5 results in the highest affinity binding to full-length Pin1. Each of the P.Ser-Pro sites in the doubly phosphorylated species contributes to the observed binding. Both P.Ser 2 and P.Ser 5 are capable of binding to the single phosphate binding site on Pin1's WW domain, and the higher apparent affinity of the doubly phosphorylated peptide can, therefore, be accounted for in part by the additive affinities of each monophosphorylated species. Furthermore, the moderate affinity of Pin1's PPIase domain for the doubly phosphorylated peptide can account for some of the additional binding energy of the doubly phosphorylated peptide for full-length Pin1.

Notably, full-length Pin1 yielded higher apparent affinities in equilibrium binding experiments than either the PPIase or WW domains alone. This experimental observation may be partly due to stabilization of the WW domain by interactions with the Pin1 PPIase domain. Furthermore, the PPIase domain in full-length Pin1 ensures that both P.Ser-Pro peptide bonds in the doubly phosphorylated Pol II CTD peptide sample the *cis* and *trans* conformational states on a fast time scale, thus affording a continuous supply of the all-*trans* peptide for association with the WW domain (see below). Finally, the partial shielding of the hydrophobic WW domain peptide binding interface from the surrounding solvent by the PPIase domain represents the physiologically relevant environment of the Pin1 interaction surface.

This limited binding analysis divides P.Ser/P.Thr-Pro peptides into two affinity groups, possibly distinguished by a second Pro residue located at the -2 position relative to P.Ser/P.Thr. To understand the phosphopeptide binding interface on a structural level, we carried out an X-ray crystallographic analysis of a Pin1–phosphopeptide complex.

Overall architecture

Crystals of Pin1 bound to Tyr-P.Ser-Pro-Thr-P.Ser-Pro-Ser were obtained from equimolar mixtures of Pin1 and the doubly phosphorylated CTD peptide. The structure was solved by molecular replacement using the published model of Pin1[19] and refined to 1.84 Å resolution. The CTD phosphopeptide resides in the cavity separating the PPIase domain from the WW domain and contacts residues on the concave surface of Pin1's WW domain (Fig. 1). The Pin1 PPIase domain does not contribute to the peptide binding interface in this crystal form. Additional complexes with longer peptides and proteins will be necessary to completely describe the contribution of each domain to target recognition.

Two conformational differences exist in the current Pin1–peptide co-crystal structure when compared to the other reported structure without a peptide bound to the WW domain[19]. The first difference resides in the PPIase domain. A 70° rotation of the β1/α1 (residues 64–80) catalytic loop results in an open conformation of the PPIase domain's active site. Arg 68 and Arg 69, which confer preferential binding of phosphorylated substrates to the Pin1 PPIase domain, now reside well outside of the proline ring binding pocket formed by His 59, Cys 113, Leu 122, Met 130, Phe 134, and His 157 (Fig. 1*a*,*b*). In this static view, a crystal packing interaction maintains this open architecture. This orientation of the β1/α1 catalytic loop likely reflects the inherent mobility of this selectivity filter in solution when not engaged with a bound phosphopeptide.

The second conformational difference occurs in the Pin1 WW domain and results in an exaggerated twist in the triple-stranded antiparallel β-sheet. This twist is coupled to a contraction of the concave WW domain ligand binding surface around the extended CTD peptide. The upper third of β2′ and β3′, together with the β2′/β3′ turn, moves downward over the N-terminal half of the CTD peptide. This movement positions Arg 14 and Phe 25 in van der Waals contact with Pro 3 of the CTD peptide and Ser 32 within hydrogen bonding distance of the backbone carbonyl oxygen of Thr 4 on the CTD peptide. The lower portions of the β1′ and β2′ strands, together with their connecting loop, pivot upward, positioning Ser 16 and Arg 17 within hydrogen bonding distance of the phosphate on P.Ser 5 of the CTD peptide. The complete phosphate binding module of the Pin1 WW domain encompasses the side chains of Ser 16, Arg 17, and Tyr 23 and the backbone amide of Arg 17. A bound water molecule mediates the hydrogen bond between Tyr 23 and the P.Ser 5 phosphate (Fig. 2*a*,*b*). The Tyr 23-Trp 34 aromatic pair spatially defines the pivot point for all of these structural changes.

The aromatic rings of these residues align edge-to-face to form a clamp that accommodates the backbone atoms of Thr 4 and P.Ser 5 and the ring atoms of Pro 6 of the CTD peptide (Fig. 1*c*). Finally, the Ser 7 side chain hydroxyl group forms a hydrogen bond with

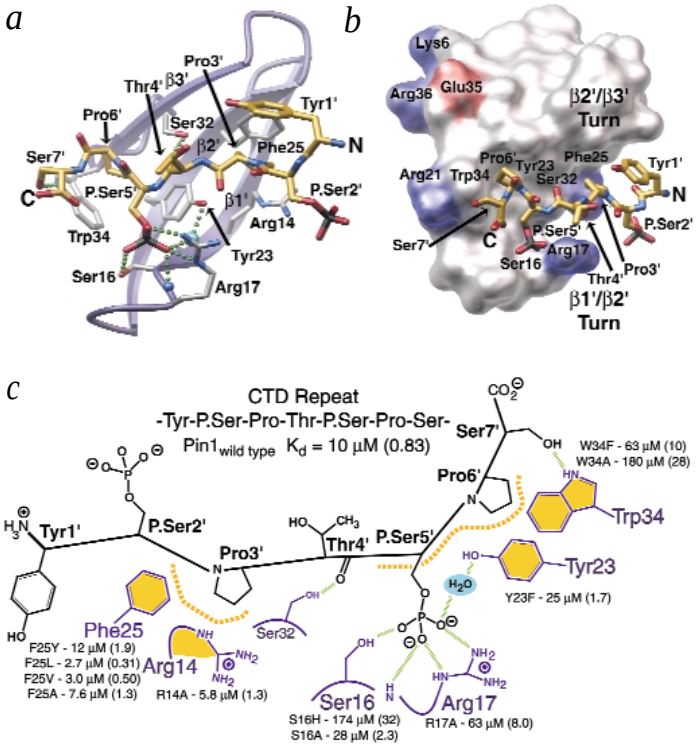

Fig. 2 The Pin1–CTD peptide binding interface. ***a***, Ribbon diagram of the Pin1 WW domain bound to Tyr-P.Ser-Pro-Thr-P.Ser-Pro-Ser depicted after a 90° rotation around a vertical axis from the view shown in Fig. 1*a*. This view is looking onto the concave WW domain peptide binding surface opposite the PPIase domain. The carbon atoms of the CTD peptide are colored gold to distinguish them from the WW domain side chain atoms. The water molecule mediating Tyr 23–phosphate contacts is shown as a cyan sphere. Hydrogen bonds are shown as green dotted spheres. ***b***, Molecular surface representation of the WW domain–peptide interface rendered after a slight rotation around the vertical axis from the view depicted in (*a*). The solvent accessible surface for the Pin1 WW domain residues was calculated in GRASP[33], and the acidic and basic residues colored red and blue, respectively. ***c***, Schematic and energetic view of the Pin1–phosphopeptide complex. Pin1 residues are purple and CTD residues black. Residues participating in van der Waals contacts are highlighted with gold and the extended van der Waals surfaces appear as dotted gold curves. Hydrogen bonds are shown as dashed green lines. In the case of the S16H and W34H mutants, some of the apparent binding is likely being contributed by the PPIase domain. Residues are given in the single letter code. Values in parentheses represent deviations from theoretical binding isotherms.

the protonated indole nitrogen of Trp 34 (Fig. 2*a*). Tyr 1 and P.Ser 2 of the CTD peptide exhibit a greater degree of flexibility, which is reflected in their weak electron density. The entire peptide binds as an extended coil, with both P.Ser-Pro peptide bonds in the *trans* configuration. Modeling of either peptide bond in the *cis* configuration results in steric perturbations at the ligand binding interface that would likely result in a loss of peptide binding. These steric factors are most pronounced around the P.Ser 5-Pro 6 segment, which is sequestered by the single phosphate binding site on the WW domain and by the Tyr 23-Trp 34 clamp. While the phosphate on P.Ser 2 is not in direct contact with the WW domain, Arg 14 and Phe 25 both restrict the P.Ser 2-Pro 3 peptide bond to the *trans* configuration (Fig. 2*b*). Shorter aliphatic side chains at either of these positions could accommodate a *cis* peptide bond at this site. This three-dimensional view supports the idea that WW domains have an extended contact surface that can recognize a maximum of five consecutive polypeptide residues.

Energetic significance of protein–peptide interactions

To investigate the energetics of the WW domain peptide binding interface, the affinities of a limited series of Pin1 mutants for the doubly phosphorylated CTD peptide were measured by fluorescence anisotropy (Fig. 2*c*). The most energetically important phosphate interaction constitutes the electrostatic contact observed crystallographically between the side chain δ-guanido group of Arg 17 and the phosphate moiety on Ser 5 of the CTD peptide. Replacement of Arg 17 by Ala results in a six-fold decrease in binding affinity. In R17A Pin1, the remaining hydrogen bonds between the phosphate on Ser 5′ and the side chain hydroxyl group of Ser 16, the backbone amide of Ala 17, and the water mediated contact with the Tyr 23 hydroxyl moiety may provide an interface for the lower affinity binding of the phosphopeptide (K_d = 63 μM).

Emericella nidulans Pin1 contains an Asn residue in place of Arg 17 (Fig. 3*a*). While neutral, the amide side chain at this position can act as a hydrogen bond donor for the P.Ser residue. Therefore, WW domains possessing neutral hydrogen bond donors at positions equivalent to 16, 17, and 23 in Pin1 may provide an energetically acceptable interface for P.Ser/P.Thr-Pro recognition. The fourth WW domain (WW4) of the HECT (homologous to E6-AP C-terminus) domain containing ubiquitin ligase WWP1 (WW domain protein 1) contains a conserved Thr-Arg segment homologous to Ser 16 and Arg 17 of Pin1 (Fig. 3*a*). Preliminary binding analysis of recombinant WW1, WW3, and WW4 of WWP1 with the doubly phosphorylated CTD peptide demonstrates phosphorylation dependent binding only to WW4 (M.A.V. and J.P.N., unpublished observations).

In addition to the group IV WW domains, several phosphoprotein binding domains exist, including Src-homology II (SH2), phosphotyrosine binding domain (PTB), STYX (phosphoserine/threonine/tyrosine-binding protein), SCB-binding factor (SBF), 14-3-3, and forkhead associated (FHA) domains[21]. These domains are each structurally distinct, but all of them utilize Arg residues for the recognition of phosphate on P.Ser, P.Thr, and P.Tyr[22–24] side chains.

Mutations of the other two side chain hydrogen bond donors, Ser 16 and Tyr 23 to Ala and Phe, respectively, each result in a 2.5-fold decrease in binding affinity. These thermodynamic measurements correlate with the observed structure of the Pin1–CTD interface and are consistent with the loss of charged and neutral hydrogen bonding residues in the R17A, S16A, and Y23F mutants. Probable steric blockage of the phosphate binding pocket by the S16H mutant significantly perturbs binding.

Trp 34 constitutes one of two conserved Trp residues found in nearly all WW domains described to date. Together with Tyr 23, this aromatic pair organizes around the Thr 4 and P.Ser 5 backbone, and Pro 6 of the CTD peptide. Replacement of Trp 34 by Phe or Ala causes a six-fold and 18-fold reduction in binding affinity, respectively. The W34A mutant result is consistent with the reduction of side chain volume at position 34 that results in a substantial shrinkage of the interaction surface with the CTD peptide's backbone and the pyrrolidine ring of Pro 6. All Pin1 homologs described to date include one additional residue in the turn linking β1′ and β2′ (Fig. 3*a*). This unique structural feature of group IV WW domains may facilitate the conformational change in the β1′/β2′ turn that is necessary for the formation of the phosphate binding pocket. Structural and energetic analysis of both deletion and insertion mutants of the β1′/β2′ loop in a set of WW domains is currently in progress.

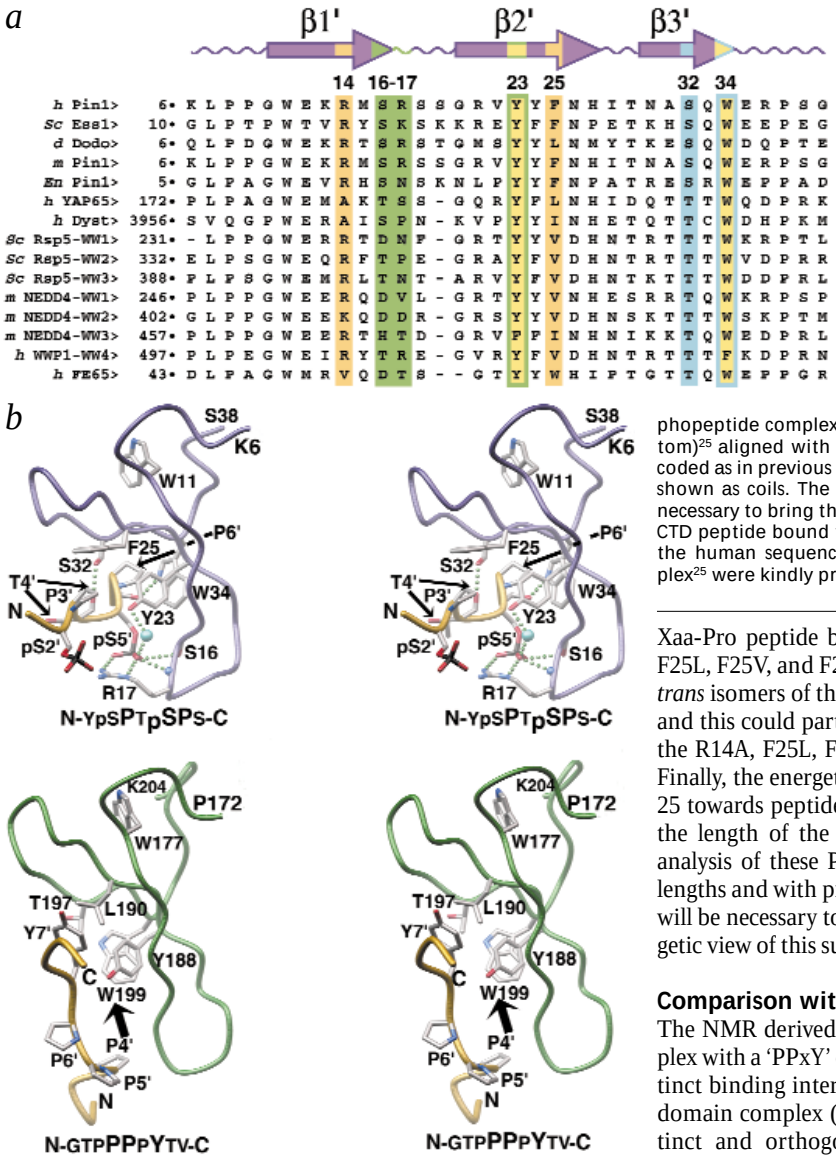

Fig. 3 Representative WW domains. ***a***, Sequence alignment of 15 WW domains. The secondary structural elements are those of Pin1. The numbers correspond to the first residue on each line for each of the 15 WW domains. Green boxes delineate residues participating in phosphate contacts. Shaded orange boxes define residues participating in van der Waals contacts with Pro 3 of the CTD peptide. Orange boxes highlight residues contributing to the van der Waals surface sequestering the backbone of residues 4–6 as well as the pyrrolidine ring of Pro 6. Light blue boxes define residues participating in additional hydrogen bonds with the CTD peptide. Residues participating in more then one class of interactions are outlined and color coded as described above. *h*, human; *Sc*, *Saccharomyces cerevisiae*; *d*, *Drosophila*; *m*, mouse; *En*, *Emericella nidulans*. ***b***, Stereo views of the Cα traces of the Pin1–phosphopeptide complex (top) and the YAP65–'PPxY' peptide complex (bottom)[25] aligned with Pin1's WW domain. The figure is labeled and color coded as in previous figures. The backbones of the WW domains are now shown as coils. The arrow in the bottom panel depicts the movement necessary to bring the 'PPxY' containing peptide into alignment with the CTD peptide bound to Pin1. The numbering scheme for YAP65 refers to the human sequence. Coordinates of the YAP65–'PPxY' peptide complex[25] were kindly provided by M. Sudol.

Surprisingly, mutations of either Arg 14 or Phe 25, which contribute to the observed binding interface, result in enhanced binding affinities when replaced with shorter chain aliphatic residues commonly found in group I WW domains. The interface formed by each of these side chains with Pro 3 of the CTD peptide is less extensive than the interface formed by the Tyr 23-Trp 34 pair surrounding Thr 4, P.Ser 5, and Pro 6 of the CTD peptide. Mutations at either position 14 or 25 would be expected to result in only modest energetic perturbations. Structural analysis of the R14A Pin1 mutant without a peptide bound to its WW domain shows that the WW domain in this mutant exists in the conformation described for the current Pin1–phosphopeptide complex rather than the conformation seen in the wild type Pin1 structure[19] (M.A.V. & J.P.N., unpublished observations). Therefore, the enhanced binding affinity observed for the R14A mutant might be due in part to stabilization of the pre-organized peptide binding interface of the Pin1 WW domain in the absence of peptide ligands.

In addition, Arg 14 and Phe 25 in wild type Pin1 impose strict selectivity for a *trans* peptide bond between P.Ser 2 and Pro 3 of the CTD peptide. In solution, Pro-containing peptides like the CTD peptide populate both the *cis* and *trans* configurations around Xaa-Pro peptide bonds. Pin1 WW domain mutants like R14A, F25L, F25V, and F25A, may be capable of binding either the *cis* or *trans* isomers of the P.Ser 2-Pro 3 and P.Ser 5-Pro 6 peptide bond, and this could partly account for the higher apparent affinities of the R14A, F25L, F25V, and F25A mutants for the CTD peptide. Finally, the energetic contribution of residues at positions 14 and 25 towards peptide and protein recognition may also depend on the length of the bound polypeptide. Structural and energetic analysis of these Pin1 mutants with bound peptides of varying lengths and with proteins capable of spanning both Pin1 domains will be necessary to provide a more complete structural and energetic view of this subset of WW domain–ligand interfaces.

Comparison with other WW domains

The NMR derived structure of the YAP65 WW domain in complex with a 'PPxY' containing peptide[25] displays a structurally distinct binding interface from that of the CTD peptide–Pin1 WW domain complex (Fig. 3*b*). While this difference may reflect distinct and orthogonal mechanisms for ligand recognition by group I and group IV WW domains, the recent structural analysis of the dystrophin WW domain in complex with a 'PPxY' containing peptide argues against this conclusion for group I and group IV WW domains[26]. Modeling the peptide bound to YAP65 in a manner similar to that observed in the Pin1–CTD complex results in a peptide orientation superimposed on the extended binding interface observed for Pin1. However, the direction of the polypeptide chain is reversed. This orientation is consistent with that of a 'PPxY' peptide bound to the dystrophin WW domain. However, even though Pin1 and dystrophin bind their respective ligands in opposite directions, apart from Pin1's ability to bind phosphopeptides, the chemical features of both peptide binding interfaces are nearly identical[26]. The capacity of WW domains to bind protein ligands in a bi-directional manner is consistent with the dystrophin WW domain structure and is reminiscent of the alternative binding modes utilized by SH3 domains[22].

Conclusion

The picture that emerges is of a rather limited WW domain contact surface that relies on a set of energetically modest side chain interactions, none of which is absolutely essential for ligand binding. Rather, the summed contributions of the WW domain

Table 2 Crystallographic data, phasing, and refinement information

Wavelength (Å)	0.98
Resolution range (Å)	62.02–1.84
Observations	293,095
Unique reflections	17,107
Completeness[1] (%)	97.3 (98.2)
I / σ[1]	21.5 (4.3)
R_{sym}[1,2] (%)	6.2 (33.7)
R_{cryst}[3] / R_{free}[4] (%)	23.1 / 27.1
Protein atoms	1,235
Water molecules	151
Peptide atoms	39
R.m.s.deviations	
Bonds (Å)	0.029
Angles (°)	2.6
Average B-factors	
Protein (Å^2)	27.3
Water (Å^2)	36.0

[1]Numbers in parentheses are for the highest resolution shell.
[2]$R_{sym} = \Sigma|I_h - \langle I_h \rangle| / \Sigma I_h$, where $\langle I_h \rangle$ is the average intensity over symmetry equivalent reflections.
[3]$R_{cryst} = \Sigma||F_o| - |F_c|| / \Sigma|F_o|$, where summation is over the data used for refinement.
[4]R_{free} was calculated using 5% of data excluded from refinement.

recognition of polypeptide ligands spanning five consecutive amino acid residues together with interactions contributed by additional modular domains and longer polypeptide targets likely contribute to target selection in WW domain containing proteins such as Pin1. This study, together with other structural[26] and functional studies of WW domains, demonstrate how the WW domain architecture provides a platform on which varying polypeptide specificities are built.

Methods

Protein purification and crystallography. His tagged Pin1 was expressed and purified by Ni^{+2}-chelation chromatography, the His tag was removed by thrombin digestion, and the protein purified as described[19]. All site directed mutants were constructed using the QuikChange (Stratagene) protocol and purified like wild type Pin1. Crystals of the Pin1–phosphopeptide complex were grown in hanging drops at 4 °C by mixing 1.0 μl of the Pin1–peptide complex with 1.0 μl of a reservoir solution containing 100 mM 3-(N-morpholino)-2-hydroxy propane sulfonic acid (MOPSO)-Na^+ (pH 7.0), 28% (v/v) PEG 8000, 2 mM dithiothreitol (DTT). The resulting crystals were stabilized in 100 mM MOPSO-Na^+ (pH 7.0), 25% (v/v) PEG 8000, 20% (v/v) glycerol, 1 mM DTT, and rapidly frozen in a 100 K stream of nitrogen gas. A native data set extending to 1.84 Å resolution was collected at the Stanford Synchrotron Radiation Laboratory, beamline 9-1 (λ = 0.98 Å). Data were processed with DENZO and scaled with SCALEPACK[27]. The crystals contain one Pin1–peptide complex per asymmetric unit and belong to space group $P2_12_12_1$ (a = 35.27 Å, b = 43.90 Å, c = 124.66 Å, α = β = γ = 90°). The structure of the Pin1–phosphopeptide complex was solved by molecular replacement using AMORE[28] and the coordinates for the previous Pin1 monomer model[19]. The resulting model was then positionally refined against all the data between 62.02 Å and 1.84 Å using the default bulk solvent model in CNS with maximum likelihood targets[29]. After refining the rebuilt model, water molecules were added automatically using CNS and edited manually in O[30]. This model consists of residues 1–38 and 51–163 of human Pin1, the entire phosphopeptide, and 151 water molecules (Table 2). Model quality was checked with PROCHECK[31]. A total of 91.7% of the residues are in the most favored regions of the Ramachandran plot, 6.8% in the additional allowed region, and 0.8% in the generously allowed region. Glu 5 borders the generously allowed region.

Binding analysis. CTD peptides were obtained commercially (SynPep Corporation). All other peptides were synthesized manually using standard procedures and purified by reverse phase chromatography. Lyophilized peptides were dissolved in 25 mM HEPES-Na^+ (pH 7.5), 100 mM NaCl, 1 mM DTT and stored for short periods of time at -20°C. Peptides were labeled with the amine reactive reagent tetramethylrhodamine-5-(and-6)-isothiocyanate (Molecular Probes, Inc. Eugene, Oregon) using a 2:1 molar ratio of rhodamine to peptide in 0.1 M sodium bicarbonate (pH 9.0) at ambient temperature for 10 h. Fluorescence data were collected on a PTI Alphascan spectrofluorimeter (Photon Technology Instruments, Santa Clara, California). Dissociation equilibrium constants for Pin1–peptide complexes were determined by measuring the change in fluorescence anisotropy of a set of peptide solutions at constant concentration of peptide, each of which contained varying concentrations of Pin1 using the procedure described[32].

Coordinates. Coordinates for the Pin1–phosphopeptide complex have been deposited in the Protein Data Bank (accession code 1F8A).

Acknowledgments
We thank members of the Noel lab and the staff of the Stanford Synchrotron Radiation Laboratory (SSRL) for assistance during data collection at beamline 9-1, R.D. Mullins and L. Blanchoin for guidance with the fluorescence measurements, and S. Richards for assistance with molecular replacement. We are especially grateful to M. Sudol and M.J. Eck for communicating their results prior to publication. The SSRL Biotechnology Program is supported by the National Institutes of Health, National Center for Research Resources, Biomedical Technology Program, and by the Department of Energy, Office of Biological and Environmental Research. This work was supported by a USPHS grant awarded to J.P.N. T.H. is a Frank and Else Schilling American Cancer Society Professor. K.P.L. is a Pew Scholar and a Leukemia Society of America Scholar.

Correspondence and requests for materials should be addressed to J.P.N. *email: noel@sbl.salk.edu*

Received 26 April 2000; accepted 28, June, 2000.

1. Sudol, M. *Prog. Biophys. Mol. Biol.* **65**, 113–132 (1996).
2. Chen, H.I., *et al. J. Biol. Chem.* **272**, 17070–17077 (1997).
3. Ermekova, K.S., *et al. J. Biol. Chem.* **272**, 32869–32877 (1997).
4. Bedford, M.T., Reed, R. & Leder, P. *Proc. Natl. Acad. Sci. USA* **95**, 10602–10607 (1998).
5. Lu, P.J., Zhou, X.Z., Shen, M.S. & Lu, K.P. *Science* **283**, 1325–1328 (1999).
6. Komuro, A., Saeki, M. & Kato, S. *J. Biol. Chem.* **274**, 36513–36519 (1999).
7. Beford, M.T., Sarbassova, D., Xu, J., Leder, P. & Yaffe, M.B. *J. Biol. Chem.* **275**, 10359–10369 (2000).
8. Crenshaw, D.G., Yang, J., Means, A.R. & Kornbluth, S. *EMBO J.* **17**, 1315–1327 (1998).
9. Shen, M., Stukenberg, P.T., Kirschner, M.W. & Lu, K.P. *Genes Dev.* **12**, 706–720 (1998).
10. Wells, N.J., *et al. J. Cell. Sci.* **112**, 3361–3371 (1999).
11. Lu, P.J., Wulf, G., Zhu, X.Z., Davies, P. & Lu, K.P. *Nature* **399**, 784–788 (1999).
12. Hani, J., *et al. J. Biol. Chem.* **274**, 108–116 (1999).
13. Albert, A., Lavoie, S. & Vincent, M. *J. Cell Sci.* **112**, 2493–2500 (1999).
14. Komuro, A., Saeki, M. & Kato, S. *Nucleic Acids Res.* **27**, 1957–1965 (1999).
15. Morris, D.P., Phatnani, H.P. & Greenleaf, A.L. *J. Biol. Chem.* **274**, 31583–31587 (1999).
16. Steinmetz, E.J. *Cell* **89**, 491–494 (1997).
17. Ho, C.K. & Shuman, S. *Mol. Cell* **3**, 405–411 (1999).
18. Chang, A., Cheang, S., Espanel, X. & Sudol, M. *J. Biol. Chem.* April 25 [epub ahead of print] (2000).
19. Ranganathan, R., Lu, K.P., Hunter, T. & Noel, J.P. *Cell* **89**, 875–886 (1997).
20. Yaffe, M.B., *et al. Science* **278**, 1957–1960 (1997).
21. Plowman, G.D., Sudarsanam, S., Bingham, J., Whyte, D. & Hunter, T. *Proc. Natl. Acad. Sci. USA* **96**, 13603–13610 (1999).
22. Kuriyan, J. & Cowburn, D. *Annu. Rev. Biophys. Biomol. Struct.* **26**, 259–288 (1997).
23. Yaffe, M., *et al. Cell* **91**, 961–971 (1997).
24. Liao, H., Byeon, I.L. & Tsai, M.D. *J. Mol. Biol.* **294**, 1041–1049 (1999).
25. Macias, M.J., *et al. Nature* **382**, 646–649 (1996).
26. Huang, X. *et al. Nature Struct. Biol.* **7**, 634–638 (2000).
27. Otwinowski, Z. & Minor, W. *Methods Enzymol.* **276**, 307–326 (1997).
28. Navaza, J. *Acta Crystallogr. A* **50**,157–163 (1994).
29. Brunger, A.T., *et al. Acta Crystallogr. D* **54**, 905–921 (1998).
30. Jones, T.A., Zou, J.Y., Cowan, S.W. & Kjeldgaard, M. *Acta Crystallogr. D* **49**, 148–157 (1993).
31. Laskowski, R.A., MacArthur, M.W., Moss, D.S. & Thornton, J.M. *J. Appl. Crystallogr.* **26**, 283–291 (1993).
32. Vinson, V.K., De La Cruz, E.M., Higgs, H.N. & Pollard, T.D. *Biochemistry* **37**, 10871–10880 (1998).
33. Nicholls, A., Sharp, K.A. & Honig, B. *Proteins* **11**, 281–296 (1991).